

# High-resolution X-ray Computed Tomography datasets of stone mastic asphalt drill cores before and after multi-step uniaxial compression creep/relaxation testing

Matthias Ruf<sup>i</sup>    Tim Teutsch<sup>ii</sup>    Stefan Alber<sup>ii</sup>  
Wolfram Ressel<sup>ii</sup>    Holger Steeb<sup>iii</sup>

2025

<https://doi.org/10.46298/jodakiss.15205>

This document is licensed under the terms of the  
Creative Commons Attribution 4.0 International License (CC BY 4.0).

<sup>i</sup>University of Stuttgart, Institute of Applied Mechanics (CE)

<sup>ii</sup>University of Stuttgart, Institute for Road and Transport Science

<sup>iii</sup>University of Stuttgart, Institute of Applied Mechanics (CE) & SC SimTech

## Abstract

Multi-step uniaxial compression creep and relaxation tests were performed on three stone mastic asphalt drill cores. Before and after the mechanical tests, micrometer resolution X-Ray Computed Tomography ( $\mu$ XRCT) imaging of the drill cores was performed to characterize the deformation and damage state of the microstructure as a result of the multi-step uniaxial compression loading tests. Both the mechanical measurement results as well as the reconstructed grayscale  $\mu$ XRCT images with a voxel size of 30  $\mu$ m are included.

## 1 Background

The microstructure of asphalt concrete has become an important area of research in pavement engineering, mainly because it can explain the main cause of pavement failure. In order to characterize asphalt structures consisting of the three basic components, coarse aggregates, mortar (binder, fine aggregates, filler) and air voids, micro X-Ray Computed Tomography ( $\mu$ XRCT) has become a prominent 3D imaging technique. It provides non-destructive access to the morphology of asphalt concrete down to micrometer resolution. Because of its non-destructive nature, it allows classical characterization methods such as mechanical testing to be combined with  $\mu$ XRCT imaging at different sample states. The three investigated drill cores in the three datasets [1, 2, 3] are stone mastic asphalt with a nominal maximum aggregate size of 11 mm. Each of the three datasets contains the measurement data of the performed multi-step uniaxial compression creep/relaxation tests and  $\mu$ XRCT images of the initial sample state and the state after the performed mechanical test.

## 2 Specification

Table 1: Specification

Subject	Engineering: Structural and Civil Engineering
Specific subject area	Asphalt structures; High-resolution micro X-ray Computed Tomography
Type of data	Table, Images (reconstructed grayscale images)
Data collection	(1) Mechanical measurements (2) micro X-ray Computed Tomography (ex situ)
Related research article	None.

### 3 Value

The dataset provided is of high value to the scientific community. The dataset can be used in different ways, such as:

- General improvement of the understanding of the morphology of asphalt concrete and its evolution in the deformed or damaged state.
- Enhancement of analysis methods of the morphology of asphalt concrete structures based on 3D image data for the intact and deformed/damaged state.
- Computational creation of artificial asphalt concrete microstructures and their improvements based on the image and measurement data.
- Enhancement of numerical and theoretical multi-scale and multi-phase (multi-X) approaches as basis for coarse-grained considerations of long-term behavior of roads.
- The dataset can be used by researchers in the fields of computational solid mechanics, computational fluid dynamics, digital porous media and image processing, among others.

### 4 Data Description

Each of the three datasets [1, 2, 3] contains the measurement results (time, displacement, load, eng. stress, and eng. strain) of multi-step uniaxial compression creep/relaxation tests (files: \*\_compression\_test\_data.csv), as well as the corresponding reconstructed  $\mu$ XRCT images of the samples before and after the mechanical loading (files: reconstructed\_\*.tar.gz). The mechanical measurements performed are shown in Figure 1. Figure 2 shows representative cross-sections of sample 2-1 before and after the mechanical testing.

### 5 Experimental Design, Materials, Methods

**Samples** The three drill cores (sample 2-1, 2-2, 2-3) in the corresponding three datasets [1, 2, 3] are stone mastic asphalt with a nominal maximum aggregate size of 11 mm. It contains diabase aggregates and a 50/70 bitumen binder. Details about the material can be found in [4]. All three considered drill cores were part of one large drill core (sample 2), taken from a test track by the “Institute of Highway Engineering (ISAC)” at the RWTH Aachen and subsequently cut into three parts (sample 2-1, sample 2-2, and sample 2-3) by the “Institute of Urban and Pavement Engineering” at the Technische Universität Dresden (TUD) for further analysis. A microstructural characterization of the initial sample states based on the  $\mu$ XRCT images can be found in [5]. In Table 2, the geometrical dimensions of the three samples before and after mechanical testing are summarized. For positioning of the samples on the sample holder/rotational stage of the  $\mu$ XRCT system, the drill cores were fixed with double-sided tape on cylindrical aluminum

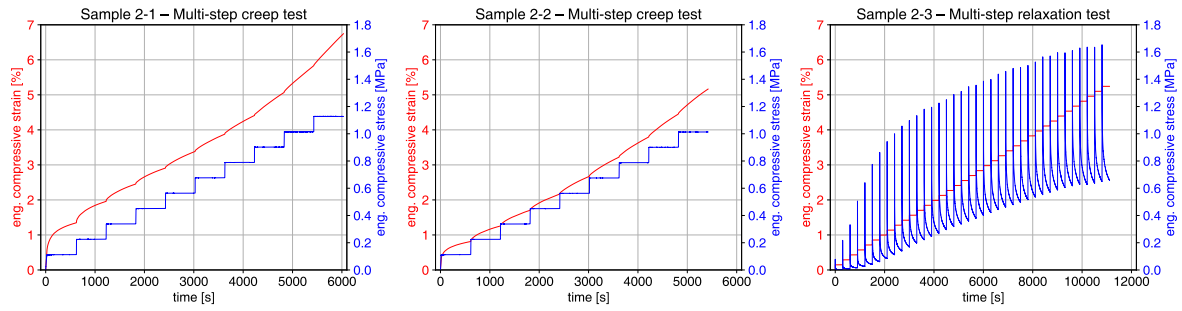


Figure 1: Visualization of the measurement data of the performed multi-step uniaxial compression creep/relaxation tests performed on the three samples.

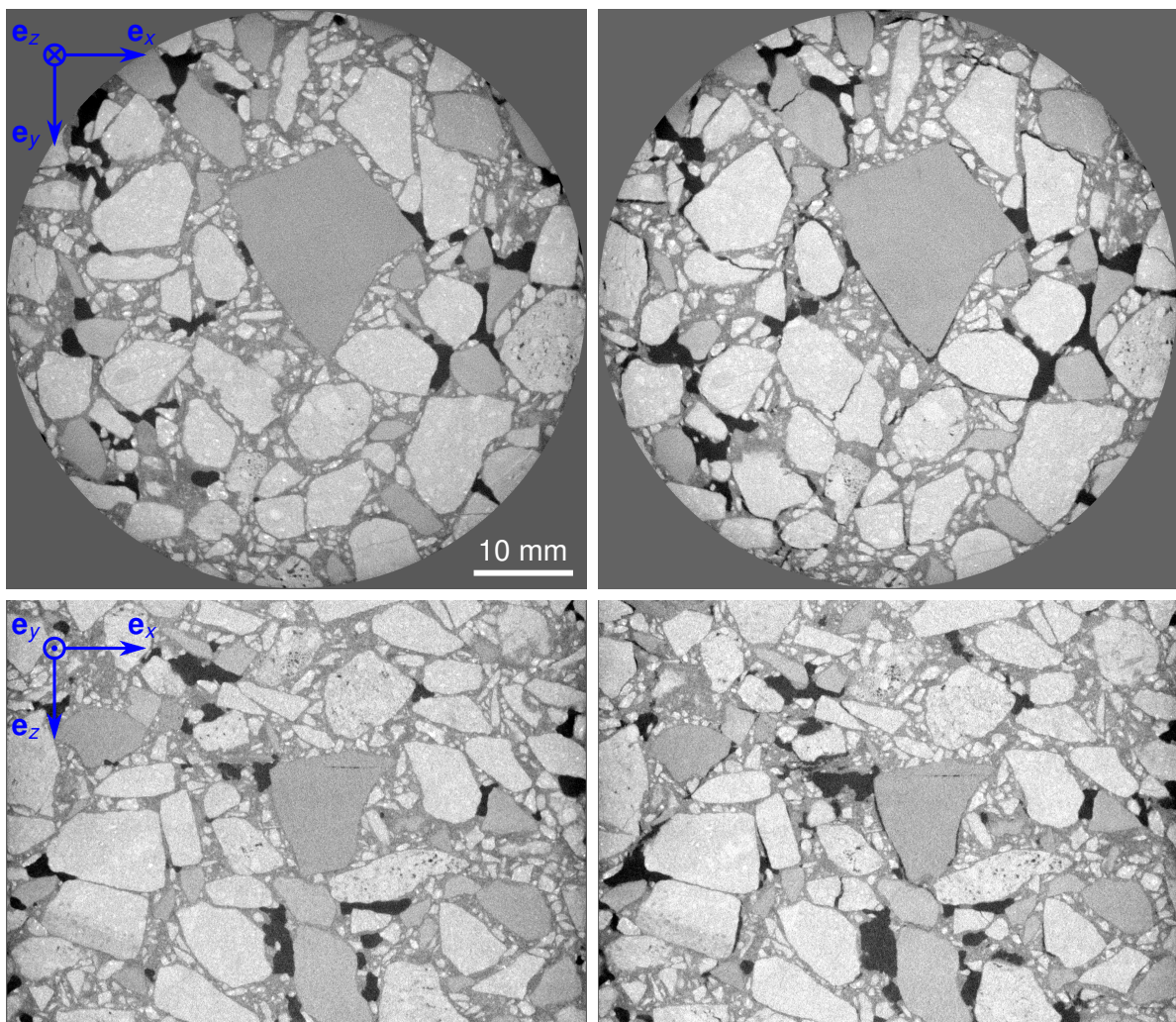


Figure 2: Visualization of  $xy$ - and  $xz$ -cross-sections of the  $\mu$ XRCT images of sample 2-1. Left: Before mechanical loading. Right: After mechanical loading.

Table 2: Sample dimensions before and after the mechanical uniaxial compression tests.

Sample	Diameter initial [mm]	Height initial [mm]	Diameter after test [mm]	Height after test [mm]
Sample 2-1	75.12	70.93	78.05	67.11
Sample 2-2	75.18	71.88	77.35	68.74
Sample 2-3	75.33	70.64	76.71	67.40

plates with a centric thread hole. The mechanical tests were performed including the aluminum plate.

**3D  $\mu$ XRCT imaging** The 3D images cover a cylindrical subregion of 58.32 mm in diameter and 42.75 mm in height located in the center of each core. The voxel size of all  $\mu$ XRCT-images is 30  $\mu$ m. A modular  $\mu$ XRCT system described in [6] was used for 3D imaging. The acquisition parameters were configured as follows: geometric magnification of 2.5, tube voltage of 160 kV, tube current of 400  $\mu$ A, projections over a rotation of 360° in 0.25° steps, frame averaging of 5 slightly shifted detector positions for bad pixel compensation, exposure time of 2000 ms for each projection. The 3D volume reconstruction was performed with the FDK algorithm [7] using the commercial software Octopus Reconstruction (v.8.9.4-64 bit) [8].

**Multi-step uniaxial compression creep/relaxation testing** The protocol/measurements are visualized in Figure 1. The engineering stress  $\sigma$  and strain  $\varepsilon$  were determined by  $\sigma = |F|/A_0$  and  $\varepsilon = |\Delta H|/H_0$ , where  $F$  is the applied/measured load,  $A_0$  is the initial cylindrical cross-sectional area,  $\Delta H$  is the change in sample height (displacement) and  $H_0$  the initial sample height. Details of the exact test parameters can be found in the metadata of the datasets [1, 2, 3]. The samples were tested under ambient (laboratory) conditions on a RM 50 kN (Schenck-Trebel) electromechanical tensile/compression testing machine. The testing machine was refurbished by DOLI Elektronik and is equipped with an EDC 580 controller and a 63 kN load sensor.

## 6 Limitations

For sample 2-1 [1] it turned out that the sample top and bottom surfaces were not exactly plane-parallel, resulting in a non-uniform transmission of the load. The first full-surface contact between the load plate and the top surface of the sample was reached at a load of 1500 N (0.338 MPa).

## 7 Technical Validation

Mechanical testing was performed on a calibrated testing machine, and imaging was performed on a well-established  $\mu$ XRCT imaging system.

## 8 Usage Notes

The  $\mu$ XRCT images are provided as grayscale image stacks in 16 bit \*.TIF file format. They can be opened with any TIF-reader, e.g., ImageJ [9] and imported as image sequence. A rescaling of the gray values might be necessary for better recognizability. Note that the before and after scans are not registered. However, care has been taken to ensure that the sample positioning in the  $\mu$ XRCT system is approximately identical. The mechanical measurement data are provided in \*.CSV file format.

## Acknowledgment

The authors acknowledge funding by the Deutsche Forschungsgemeinschaft (DFG, German Research Foundation) through the Research Unit FOR 2089 under grant [RE 1620/4] (DFG 239224712) and support for this work within the Collaborative Research Center 1313 (DFG 327154368).

## Competing Interests

The authors declare that they have no known competing financial interests or personal relationships that could have appeared to influence the work reported in this paper.

## References

- [1] Ruf, M., Teutsch, T., Alber, S., Steeb, H., & Ressel, W. (2021). *micro-XRCT data sets of a stone mastic asphalt drill core before and after a uniaxial compression test (sample 2): sample 2-1*. DaRUS. <https://doi.org/10.18419/darus-1641>
- [2] Ruf, M., Teutsch, T., Alber, S., Steeb, H., & Ressel, W. (2021). *micro-XRCT data sets of a stone mastic asphalt drill core before and after a uniaxial compression test (sample 2): sample 2-2*. DaRUS. <https://doi.org/10.18419/darus-1833>
- [3] Ruf, M., Teutsch, T., Alber, S., Steeb, H., & Ressel, W. (2021). *micro-XRCT data sets of a stone mastic asphalt drill core before and after a uniaxial compression test (sample 2): sample 2-3*. DaRUS. <https://doi.org/10.18419/darus-1834>

- [4] Hu, J., Lui, P., & Steinauer, B. (2017). A study on fatigue damage of asphalt mixture under different compaction using 3D-microstructural characteristics. *Frontiers of Structural and Civil Engineering*, 11, 329–337. <https://doi.org/10.1007/s11709-017-0407-9>
- [5] Teutsch, T., Gönninger, L., Ruf, M., Steeb, H., & Ressel, W. (2023). Microstructural characterisation and analysis of coarse aggregates in asphalt drill cores. *Road Materials and Pavement Design*, 24(11), 1–23. <https://doi.org/10.1080/14680629.2022.2164333>
- [6] Ruf, M., & Steeb, H. (2020). An open, modular, and flexible micro X-ray computed tomography system for research. *Review of Scientific Instruments*, 91(11), 113102. <https://doi.org/10.1063/5.0019541>
- [7] Feldkamp, L. A., Davis, L. C., & Kress, J. W. (1984). Practical cone-beam algorithm. *Journal of the Optical Society of America A*, 1(6), 612–619. <https://doi.org/10.1364/josaa.1.000612>
- [8] Vlassenbroeck, J., Dierick, M., Masschaele, B., Cnudde, V., Hoorebeke, L. V., & Jacobs, P. (2007). Software tools for quantification of X-ray microtomography at the UGCT. *Nuclear Instruments and Methods in Physics Research Section A: Accelerators, Spectrometers, Detectors and Associated Equipment*, 580(1), 442–445. <https://doi.org/10.1016/j.nima.2007.05.073>
- [9] Schneider, C. A., Rasband, W. S., & Eliceiri, K. W. (2012). NIH Image to ImageJ: 25 years of image analysis. *Nature Methods*, 9(7), 671–675. <https://doi.org/10.1038/nmeth.2089>